Mon. Not. R. Astron. Soc. **363,** 555–562 (2005) doi:10.1111/j.1365-2966.2005.09459.x

The cooling of Akmal–Pandharipande–Ravenhall neutron star models

M. E. Gusakov,[1⋆] A. D. Kaminker,[1⋆] D. G. Yakovlev,[1⋆] and O. Y. Gnedin[2⋆]
[1]*Ioffe Physical Technical Institute, Politekhnicheskaya 26, 194021 Saint-Petersburg, Russia*
[2]*Ohio State University, 760 1/2 Park Street, Columbus, OH 43215, USA*

Accepted 2005 July 21. Received 2005 July 9; in original form 2005 May 10

ABSTRACT

We study the cooling of superfluid neutron stars whose cores consist of nucleon matter with the Akmal–Pandharipande–Ravenhall (APR) equation of state. This equation of state opens the powerful direct Urca process of neutrino emission in the interior of most massive neutron stars. Extending our previous recent studies (Papers I and II), we employ phenomenological density-dependent critical temperatures $T_{\rm cp}(\rho)$ of strong singlet-state proton pairing (with the maximum $T_{\rm cp}^{\rm max} \sim 7 \times 10^9$ K in the outer stellar core) and $T_{\rm cnt}(\rho)$ of moderate triplet-state neutron pairing (with the maximum $T_{\rm cnt}^{\rm max} \sim 6 \times 10^8$ K in the inner core). Choosing the position of $T_{\rm cnt}^{\rm max}$ properly, we can obtain a representative class of massive neutron stars whose cooling is intermediate between the cooling enhanced by neutrino emission due to Cooper pairing of neutrons in the absence of the direct Urca process and the very fast cooling provided by the direct Urca process non-suppressed by superfluidity.

Key words: dense matter – stars: neutron.

1 INTRODUCTION

The fundamental properties of supranuclear matter in the cores of neutron stars, such as the equation of state and critical temperatures of baryon superfluidity, are still poorly known. In particular, they can be studied (e.g. Yakovlev & Pethick 2004 and references therein) by comparing the theory of cooling isolated neutron stars with observations of thermal radiation (e.g. Pavlov, Zavlin & Sanwal 2002; Pavlov & Zavlin 2003) from these stars.

In this paper we study the cooling of superfluid neutron stars with cores composed of neutrons, protons, electrons and muons. We employ model equations of state (EOSs) of neutron star cores based on the EOS of Akmal, Pandharipande & Ravenhall (1998) (APR, Section 4), which is currently assumed to be the most elaborate EOS. It opens the powerful direct Urca process of neutrino emission (Lattimer et al. 1991) in neutron stars with masses slightly lower than the maximum mass. Our cooling models will be based on the standard (nucleon) composition of neutron stars and standard neutrino processes (no 'exotic' physics involved).

The paper extends our previous studies (Gusakov et al. 2004a; Kaminker et al. 2005; hereafter Papers I and II, respectively) of cooling neutron stars with superfluid nucleon cores, where the direct Urca process is forbidden. In this scenario, observations of cold neutron stars (e.g. of the Vela pulsar) are explained by enhanced neutrino emission due to Cooper pairing of neutrons in neutron star cores. Page et al. (2004), who suggested a similar cooling scenario, called it 'minimal cooling'. Note, however, that the realization of this scheme by Page et al. and in Papers I and II is different (see Paper II for details).

In Papers I and II we employed the EOS of Douchin & Haensel (2001) (the DH EOS, which forbids the direct Urca process in all stars) and a model of triplet-state neutron pairing with the maximum of the critical temperature $T_{\rm cnt}^{\rm max} \approx 6 \times 10^8$ K in the inner stellar core. This pairing is needed to produce an enhanced neutrino cooling of massive stars and to explain the observations of neutron stars coldest for their age (such as the Vela pulsar). In Paper I we assumed also strong singlet-state proton pairing in the outer stellar core, with $T_{\rm cp}^{\rm max} \gtrsim 5 \times 10^9$ K. It slows down the cooling of low-mass neutron stars and enables us to interpret the observations of stars warmest for their age (e.g. RX J0822−4300 or PSR B1055−52). In Paper II we included the effects of surface (accreted) envelopes of light elements. They allowed us to explain the observations of warmest stars assuming weaker proton pairing ($T_{\rm cp}^{\rm max} \gtrsim 10^9$ K).

Now we will add the effect of the direct Urca process in most massive stars in accordance with the APR EOS. We will use similar (but slightly different) models for strong proton pairing and moderate neutron pairing in the stellar core. These superfluid models are sufficient to explain current observations of all cooling neutron stars without opening the direct Urca process. However, most massive stars predicted by the APR EOS can be much colder than the stars observed today and we will focus on their properties. For simplicity, we will neglect the effects of accreted envelopes. They are unimportant for massive neutron stars; we could easily include them as in Paper II.

⋆E-mail: gusakov@astro.ioffe.ru (MEG); kam@astro.ioffe.ru (ADK); yak@astro.ioffe.ru (DGY); ognedin@astronomy.ohio-state.edu (OYG)

Table 1. Observational limits on surface temperatures of isolated neutron stars.

Source	t (kyr)	T_s^∞ (MK)	Confidence of T_s^∞ (per cent)	References
PSR J0205+6449 (in 3C 58)	0.82	$<1.02^b$	99.8	Slane et al. (2004)
Crab	1	$<2.0^b$	99.8	Weisskopf et al. (2004)
RX J0822−4300	2–5	1.6–1.9^a	90	Zavlin, Trümper & Pavlov (1999)
1E 1207.4−5209	3–20	1.4–1.9^a	90	Zavlin, Pavlov & Sanwal (2004)
RX J0007.0+7303 (in CTA 1)	10–30	$<0.66^b$	–	Halpern et al. (2004)
Vela	11–25	0.65–0.71^a	68	Pavlov et al. (2002)
PSR B1706−44	∼17	$0.82^{+0.01}_{-0.34}{}^a$	68	McGowan et al. (2004)
PSR J0538+2817	30 ± 4	$\sim 0.87^a$	–	Zavlin & Pavlov (2004)
Geminga	∼340	$\sim 0.5^b$	–	Kargaltsev et al. (2005)
RX J1856.4−3754	∼500	<0.65	–	see Paper I
PSR B1055−52	∼540	$\sim 0.75^b$	–	Pavlov & Zavlin (2003)
RX J0720.4−3125	∼1300	$\sim 0.51^a$	–	Motch et al. (2003)

[a]Inferred using a hydrogen atmosphere model. [b]Inferred using the blackbody spectrum.

2 OBSERVATIONS

Table 1 summarizes the observations of isolated (cooling) middle-aged neutron stars ($10^3\,\mathrm{yr} \lesssim t \lesssim 10^6\,\mathrm{yr}$), whose thermal surface radiation has been detected or constrained. We present the estimated stellar ages t and the effective surface temperatures T_s^∞ (redshifted for a distant observer). The data are described in Paper I and slightly corrected in Paper II.

The surface temperatures of some sources (labelled by [a]) have been obtained by fitting their thermal radiation spectra with hydrogen atmosphere models. Such models are more consistent with other information on these sources (e.g. Pavlov & Zavlin 2003) than the blackbody model. For other sources (e.g. for Geminga and PSR B1055−52, labelled by [b]), we present the values of T_s^∞ inferred using the blackbody spectrum because this spectrum is more consistent for these sources. The surface temperature of RX J1856.4−3754 is still uncertain. Following Paper I we adopt the upper limit $T_s^\infty < 0.65$ MK. Finally, T_s^∞ for RX J0720.4−3125 is taken from Motch, Zavlin & Haberl (2003), who interpreted the observed spectrum with a model of a hydrogen atmosphere of finite depth.

Note also new results by Kargaltsev et al. (2005) for Geminga presented in Table 1. As in Papers I and II we retain 20 per cent error bars for this source.

3 COOLING WITHOUT THE DIRECT URCA PROCESS

We will simulate neutron star cooling using our general relativistic cooling code (Gnedin, Yakovlev & Potekhin 2001), which calculates cooling curves (the dependence of T_s^∞ on the stellar age t). At the initial cooling stage ($t \lesssim 100$ yr) a star cools via neutrino emission but the stellar interior is non-isothermal. At the next stage ($10^2\,\mathrm{yr} \lesssim t \lesssim 10^5\,\mathrm{yr}$) the neutrino emission dominates but the interior is isothermal. Later ($t \gtrsim 10^5$ yr) the star cools mainly via surface photon emission.

For the adopted EOSs, all constituents of dense matter (nucleons, electrons and muons) exist everywhere in the stellar core, except for muons, which appear at $\rho \sim 2.0 \times 10^{14}$ g cm^{-3}. As in Paper I we use the relation between the effective surface temperature and the temperature at the bottom of the heat-blanketing iron envelope calculated by Potekhin et al. (2003).

Neutron star cooling is strongly affected by superfluidity of nucleons in stellar interiors. Any superfluidity is characterized by a density-dependent profile of critical temperature $T_c(\rho)$. In principle, an EOS and a superfluidity model, employed in cooling simulations, have to be obtained from the same nuclear Hamiltonian. However, such calculations are currently absent and one usually treats the EOS and superfluid properties as independent. Although this approach is simplified, it sounds reasonable at the present stage of the investigation because the EOS is a bulk property of the matter (determined by the entire Fermi sea of baryons) while superfluidity is a Fermi-surface phenomenon and therefore can be relatively independent. Microscopic theories predict two main types of superfluidity inside the neutron star core: singlet-state proton pairing ($T_c = T_{cp}$) and triplet-state neutron pairing ($T_c = T_{cnt}$). These theories give a large scatter of critical temperatures depending on the nucleon–nucleon interaction model and many-body theory employed (e.g. Yakovlev, Levenfish & Shibanov 1999; Lombardo & Schulze 2001; see also recent papers by Schwenk & Friman 2004; Takatsuka & Tamagaki 2004; Zuo et al. 2004; Tanigawa, Matsuzaki & Chiba 2004). As in Papers I and II, we will treat $T_{cp}(\rho)$ and $T_{cnt}(\rho)$ as phenomenological functions of ρ which do not contradict some microscopic calculations. These functions could be (in principle) constrained by comparing theoretical cooling curves with observations.

Superfluidity of nucleons affects the nucleon heat capacity and suppresses neutrino processes involving superfluid nucleons: Urca and nucleon–nucleon bremsstrahlung processes (as reviewed, for example, by Yakovlev et al. 1999). Moreover, superfluidity induces an additional neutrino emission mechanism associated with Cooper pairing of nucleons (Flowers, Ruderman & Sutherland 1976). All these effects of superfluidity are included into our cooling code in the same manner as in Papers I and II.

In Fig. 1 we plot two models of nucleon pairing employed in the present paper: model p for strong singlet-state proton pairing (with the peak of $T_{cp}(\rho)$ approximately equal to $T_{cp}^{max} \approx 6.8 \times 10^9$ K); and model nt for moderate triplet-state neutron pairing ($T_{cnt}^{max} \sim 6 \times 10^8$ K). Models p and nt differ slightly from similar models p1 and nt1 in Papers I and II. Note that the curves $T_{cp}(\rho)$ and $T_{cnt}(\rho)$ are almost insensitive to the employed EOS: DH (Papers I and II) and APR I, II and III (Section 4). Our pairing model nt seems specific (shifted to too high densities ρ at which neutron pairing dies out according to many microscopic calculations). However, similar models have been obtained from microscopic theories (e.g. see the curve $m^* = 0.73$ in fig. 1 of Takatsuka & Tamagaki 1997).

Fig. 2 illustrates the cooling scenario of Paper I (to be compared with new scenarios). We plot a family of cooling curves calculated

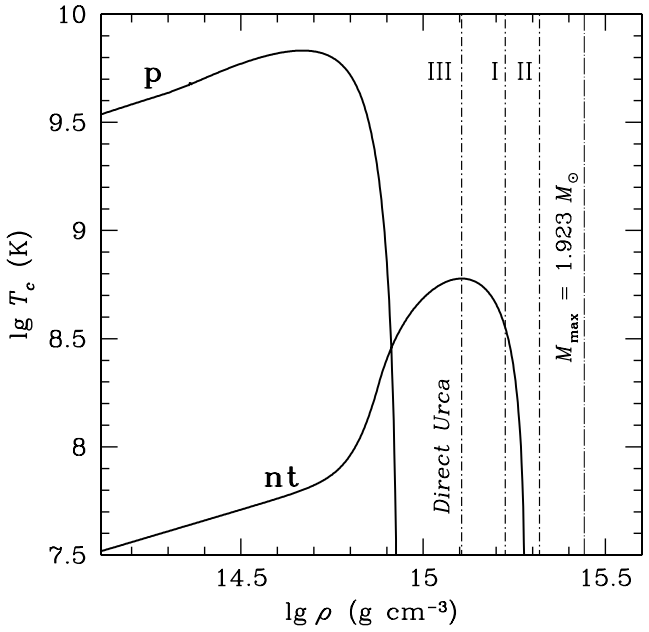

Figure 1. Density dependence of the critical temperatures for model p of singlet-state proton pairing and model nt of triplet-state neutron pairing in a neutron star core. The three vertical short-dashed/dotted lines indicate the thresholds of the direct Urca process for the EOSs APR I, II and III discussed in Section 4. The vertical long-dashed/dotted line shows the central density of a maximum-mass neutron star for APR I; the two other maximum-mass lines are almost the same.

for the DH EOS, which forbids the direct Urca process in all stable neutron stars ($M \leqslant M_{\rm max} = 2.05\,{\rm M}_\odot$). The curves refer to neutron stars with (gravitational) masses M from 1.00 to 2.04 $\rm M_\odot$ (from top to bottom).

The curves explain all the data from Table 1. The coldest objects can be interpreted as most massive neutron stars with moderate neutron pairing in the inner cores (at densities $\rho \gtrsim 8 \times 10^{14}\,{\rm g\,cm^{-3}}$). When the internal temperature of a massive star falls below $T_{\rm cnt}^{\rm max}$, the cooling is noticeably enhanced by neutrino emission due to Cooper pairing of neutrons. This enhancement is sufficient to explain the observations of neutron stars coldest for their age, particularly, PSR J0205+6449, RX J0007.0+7303, the Vela and Geminga pulsars. Note that the data on RX J0007.0+7303 are explained in this way only marginally. However, taking into account that the real uncertainties of $T_{\rm s}^{\infty}$ and t can be larger than the adopted ones, we can accept this explanation as successful. All stars with central density higher than the density at which neutron pairing dies out ($\rho_{\rm c} \gtrsim 2 \times 10^{15}\,{\rm g\,cm^{-3}}$ in Fig. 1) cool nearly as fast as the star with $M = M_{\rm max}$. This gives the lower dense bunch of cooling curves of massive neutron stars (with $\rho_{\rm c} \gtrsim 2 \times 10^{15}\,{\rm g\,cm^{-3}}$) in Fig. 2.

There is another (upper) dense bunch of cooling curves of low-mass stars ($M \lesssim 1.1\,{\rm M}_\odot$). The central densities of such stars are $\rho_{\rm c} \lesssim 8 \times 10^{14}\,{\rm g\,cm^{-3}}$. Proton pairing is strong ($T_{\rm cp}(\rho) \gtrsim 3 \times 10^9$ K) everywhere in their cores (Fig. 1). It completely suppresses all neutrino processes involving protons and substantially slows down the cooling.

Finally, there is a class of medium-mass neutron stars that show intermediate cooling. Their cooling curves fill in the space between the upper dense bunch of cooling curves (low-mass stars) and the

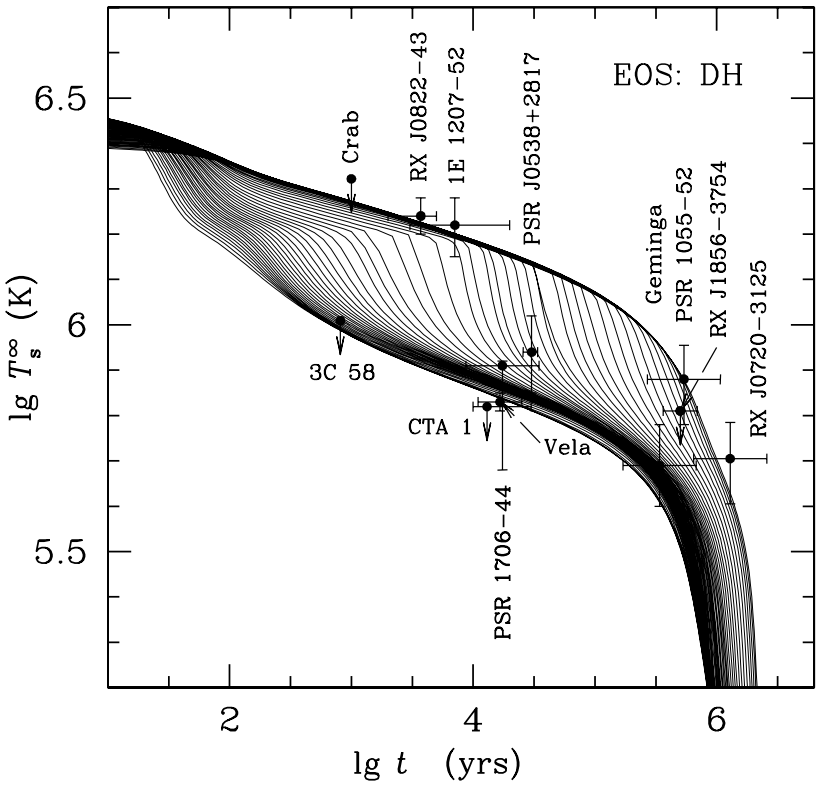

Figure 2. Observational limits on surface temperatures of 12 isolated neutron stars (Table 1) compared with theoretical cooling curves calculated for the DH EOS (no direct Urca process) and for models p and nt of nucleon pairing (Fig. 1). The 53 curves drawn refer to neutron stars of masses from 1.00 to 2.04 $\rm M_\odot$ (from top to bottom, with step 0.02 $\rm M_\odot$).

lower dense bunch (high-mass stars). We can treat PSR B1706−44, PSR J0538+2817 and RX J1856.4−3754 as medium-mass stars.

Although this scenario is consistent with all current observations, colder stars could be detected in the future. Indirect evidence for the existence of such stars is given by the non-detection of compact central objects in four supernova remnants (Kaplan et al. 2004). If neutron stars are present there, they should be really cold. It would be impossible to explain them with the cooling scenario presented in Fig. 2, but they could be interpreted adopting the APR EOS.

4 COOLING OF APR NEUTRON STARS

4.1 Equations of state

Let us employ three EOSs of dense matter, APR I, II and III. They represent a useful parametrization of the well-known EOS obtained by Akmal et al. (1998) (model Argon V18 + δv + UIX*). This parametrization was proposed by Heiselberg & Hjorth-Jensen (1999). We use the same parameters for the compressional modulus of the nucleon matter and vary only the parameter γ in the expression for symmetry energy, $S(n_b) = S_0(n_b/n_0)^\gamma$, where $S_0 = 32$ MeV, n_b is the baryon number density, and $n_0 = 0.16\,\mathrm{fm}^{-3}$ is the baryon number density in saturated nuclear matter. Specifically, we have taken $\gamma = 0.6$, 0.575 and 0.643 for the EOSs APR I, II and III, respectively. These EOSs differ mainly in the threshold densities for opening the direct Urca process (see Fig. 1).

Some properties of the EOSs and associated neutron star models are illustrated in Figs 1 and 3 and in Table 2. For comparison, in Fig. 3 and Table 2 we include also the data on the DH EOS (Douchin & Haensel 2001) and the original APR EOS (Akmal et al. 1998). The APR EOS corresponds to nucleon matter with the appearance of neutral pion condensation. To plot this EOS in Fig. 3 we use the parametrization proposed by Haensel & Potekhin (2004), with the values of fitting parameters provided by A. Y. Potekhin (private communication).

Table 2 gives masses M, central densities ρ_c and circumferential radii R of two stellar configurations. The first configuration is the most massive stable neutron star. The values of M_{max} indicate that all five EOSs are moderately stiff and similar. The second configuration refers to the onset of the direct Urca process ($\rho_c = \rho_D$, $M = M_D$); it is absent for the DH EOS. The APR III EOS implies larger symmetry energy at supranuclear densities (larger γ) and larger proton fraction than the EOSs APR I and II. Accordingly, the direct Urca process opens at lower density for APR III.

Fig. 3 shows the pressure–density (left) and the mass–central density (right) diagrams for all five EOSs. According to the left panel, all EOSs are similar. The $P(\rho)$ curves intersect at one point, $\rho \simeq 8.5 \times 10^{14}\,\mathrm{g\,cm^{-3}}$. However, small differences in the EOSs lead to noticeable differences in neutron star configurations, particularly, in the mass–density relations $M(\rho_c)$ (right panel). Corresponding proton fractions and direct Urca thresholds are also different (Table 2 and Fig. 1).

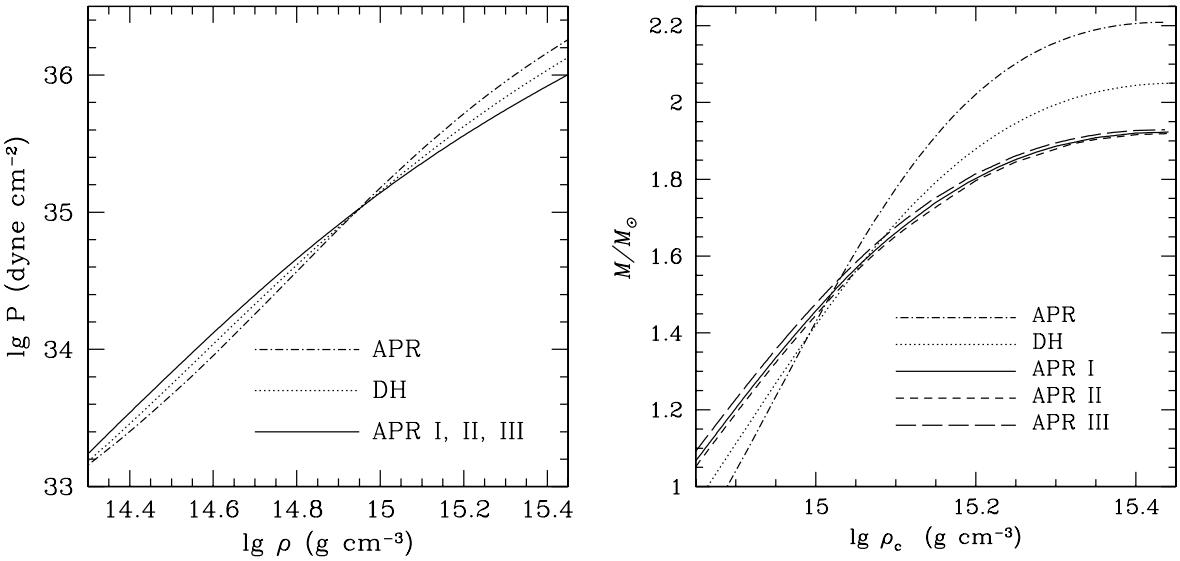

Figure 3. Pressure–density (left) and mass–central density (right) diagrams for five EOSs. The APR EOS was suggested by Akmal et al. (1998). The EOSs APR I, II and III refer to different values of γ (see Table 2) in the parametrization proposed by Heiselberg & Hjorth-Jensen (1999). The DH EOS was derived by Douchin & Haensel (2001).

Table 2. Neutron star models for the EOSs DH, APR, and APR I, II and III.

Model	Main parameters	DH	APR	APR I $\gamma = 0.6$	APR II $\gamma = 0.575$	APR III $\gamma = 0.643$
Maximum	$M_{max}/M_\odot$	2.05	2.20	1.923	1.919	1.929
mass	$\rho_{max}/10^{15}\,\mathrm{g\,cm^{-3}}$	2.86	2.74	2.759	2.774	2.731
model	R/km	9.99	9.99	10.32	10.28	10.39
Direct Urca	$M_D/M_\odot$	–	2.01	1.829	1.891	1.685
threshold	$\rho_D/10^{15}\,\mathrm{g\,cm^{-3}}$	–	1.56	1.680	2.084	1.275
model	R/km	–	10.95	11.27	10.83	11.83

4.2 Beyond the direct Urca threshold

In contrast to the cooling scenarios in Papers I and II, we use the EOS that opens the direct Urca process in massive neutron stars. Moreover, contrary to our older cooling scenarios (e.g. Kaminker, Yakovlev & Gnedin 2002; Yakovlev & Pethick 2004 and references therein), the direct Urca process is now open at densities at which proton superfluidity dies out (Fig. 1), in agreement with some recent calculations of proton pairing in dense matter (e.g. Takatsuka & Tamagaki 1997, 2004; Zuo et al. 2004).

Fig. 4 shows a family of cooling curves similar to those in Fig. 2. It is calculated for the same models of proton and neutron pairing (p and nt, Fig. 1) but adopting the APR I EOS. The curves show the cooling of neutron stars with masses from 1.01 to $M_{\rm max} = 1.92\,{\rm M}_\odot$. The density of cooling curves reflects the probability of detecting such stars provided the mass distribution of stars is flat in the indicated mass range (and observational selection effects are absent). Stars with $M \leqslant M_{\rm D} = 1.83\,{\rm M}_\odot$ would have temperatures nearly in the same range as in Fig. 2 (see Section 3). By opening the direct Urca we get a new but rare population of very cold neutron stars ($M_{\rm D} \leqslant M \leqslant M_{\rm max}$). Taking into account the difficulties of detecting such stars, the chances of observing them are really low. Notice that if the EOS would allow higher $M_{\rm max}$, we could obtain a new dense bunch of curves for very cold stars with $M \approx M_{\rm max}$.

The same effects are demonstrated in Fig. 5. It shows $T_{\rm s}^{\infty}$ versus M (left) or $\rho_{\rm c}$ (right) for stars of the Vela pulsar age, $t = 1.66 \times 10^4$ yr. We present the curves for superfluid stars with the EOSs APR I, II, and III. The horizontal dotted lines give the observational limits of $T_{\rm s}^{\infty}$ for the Vela pulsar.

One can see a very sharp fall of $T_{\rm s}^{\infty}$ in the narrow mass range from $M = M_{\rm D}$ to $M = M_{\rm D} + 0.01\,{\rm M}_\odot$ for the APR I EOS and especially for APR II. This fall is naturally associated with the strong enhancement of the neutrino luminosity by the direct Urca process.

The case of ARP III is different. As seen in Fig. 1, the threshold of opening the direct Urca process is placed now in a wide region near the maximum of the critical temperature $T_{\rm cnt}(\rho)$. When the internal stellar temperature falls noticeably below $T_{\rm cnt}(\rho)$ in some region of $\rho > \rho_{\rm D}$, the suppression of the direct Urca process by neutron superfluidity becomes important and smears out the dependence of $T_{\rm s}^{\infty}$ on M. The similar effect of partial suppression of the direct Urca process by superfluidity was discussed by Page & Applegate (1992). Evidently, the level of this suppression is regulated by the strength and density range of neutron pairing and by the threshold density of the direct Urca process. Were neutron superfluidity absent (the thin long-dashed line in Fig. 5), the dependence would be as sharp as for the EOSs ARP I and II.

The dependence of $T_{\rm s}^{\infty}$ on $\rho_{\rm c}$ (right panel of Fig. 5) is similar to the dependence on M. Note only the much smoother dependence of $T_{\rm s}^{\infty}$ on $\rho_{\rm c}$ in the lower parts of the curves; small variations of $M \lesssim M_{\rm max}$ correspond to larger variations of $\rho_{\rm c}$ (Fig. 3).

Fig. 6 is similar to Figs 2 and 4 and shows cooling curves calculated for the APR III EOS and the same models for proton and neutron pairing (p and nt). Neutron star masses range from 1.01 to $M_{\rm max} = 1.93\,{\rm M}_\odot$. The sharp lower boundary of the densely covered domain corresponds to the direct Urca threshold $M_{\rm D} = 1.68\,{\rm M}_\odot$. In contrast to Fig. 4, we now obtain a representative (densely populated) family of middle-aged neutron stars with $M > M_{\rm D}$ and $\lg T_{\rm s}^{\infty} \approx 5.6$–$5.7$. They are much colder than stars with

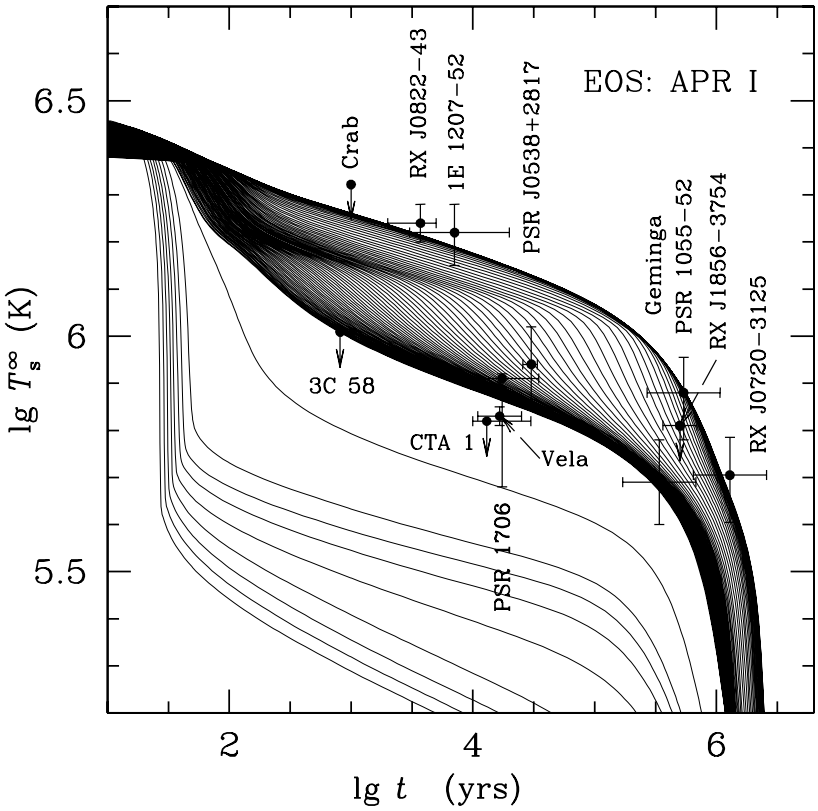

Figure 4. Same as Fig. 2 but for the EOS APR I. The 92 cooling curves drawn refer to neutron stars of masses from 1.01 to $M_{\rm max} = 1.92\,{\rm M}_\odot$ (with step $0.01\,{\rm M}_\odot$). The sharp boundary between densely and rarely covered domains corresponds to the direct Urca threshold, $M_{\rm D} = 1.83\,{\rm M}_\odot$ (Table 2).

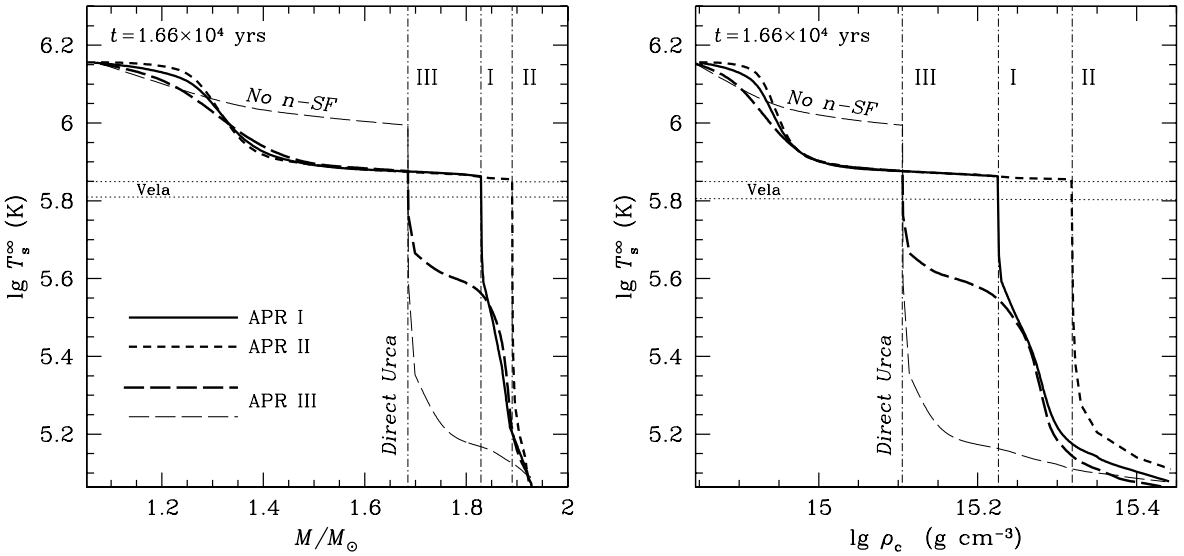

Figure 5. Surface temperatures of neutron stars of the age of the Vela pulsar, $t = 1.66 \times 10^4$ yr, versus stellar mass (left) and central density (right) for three EOSs (Table 2): APR I (solid lines), APR II (short dashes) and APR III (thin and thick long dashes), assuming either combined proton and neutron (p and nt) pairing in stellar cores (thick lines) or only proton pairing alone (No n-SF; thin lines). The vertical dashed/dotted lines, denoted I, II and III, show the threshold masses $M_{\rm D}$ (left) or densities $\rho_{\rm D}$ (right) for the direct Urca process. Horizontal dotted lines are observational limits on the surface temperature of Vela.

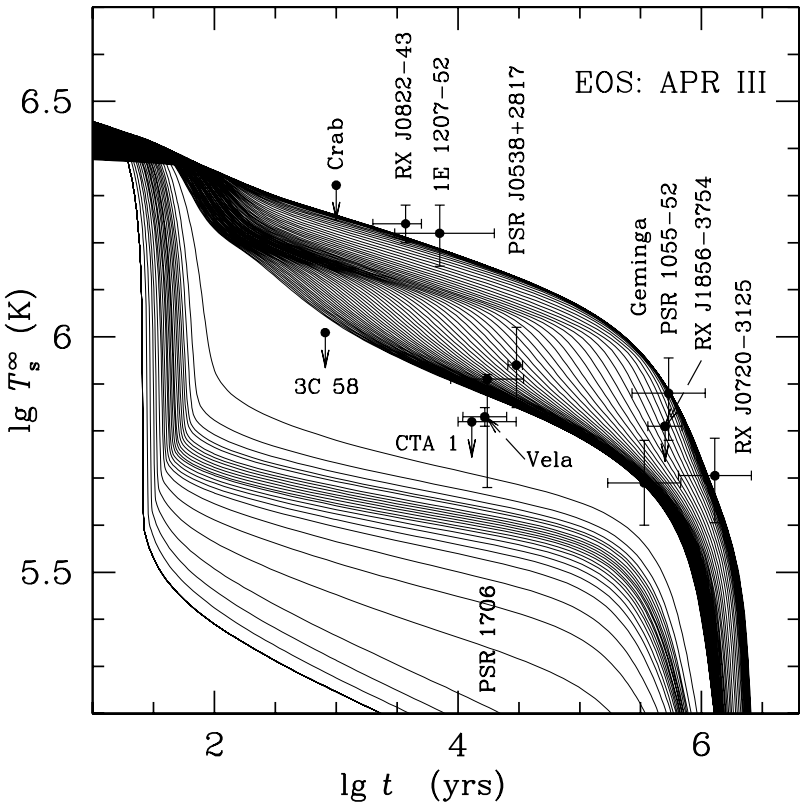

Figure 6. Same as Figs 2 and 4 but for the APR III EOS. The 93 solid curves drawn refer to neutron stars of masses from 1.01 to $M_{\rm max} = 1.93\,{\rm M}_\odot$ (with step $0.01\,{\rm M}_\odot$). The lower boundary of the densely covered domain refers to the direct Urca threshold, $M_{\rm D} = 1.68\,{\rm M}_\odot$.

$M < M_{\rm D}$ but much hotter than those with $M \approx M_{\rm max}$. They appear as a result of the flattening of the dependence $T_{\rm s}^\infty$ on M by neutron superfluidity (Fig. 5). Were this cooling scenario realized in nature, the chances of detecting such stars would be higher than for the scenario in Fig. 4.

The comparison of Figs 4 and 6 shows a slight increase of the gap between the lower boundary $T_{\rm s}^\infty(t)$ of the densely populated family of neutron stars with $M < M_{\rm D}$ and the observed surface temperature of the Vela pulsar. This difference is also illustrated in Fig. 5; the curves $T_{\rm s}^\infty(M)$ and $T_{\rm s}^\infty(\rho_{\rm c})$ merge into nearly the same

slowly decreasing function before the direct Urca thresholds ($M < M_{\rm D}$, $\rho_{\rm c} < \rho_{\rm D}$).

5 DISCUSSION AND CONCLUSIONS

We have extended the scenario of neutron star cooling proposed in Papers I and II to the class of EOSs that allow the operation of the powerful direct Urca process in the cores of massive stars. It widens the possible interpretations of observational data on thermal emission from isolated middle-aged neutron stars using the simplest models of neutron star cores composed of nucleons, electrons and muons.

The main common feature of our present scenario and the scenarios of Papers I and II is that enhanced neutrino emission, required for the interpretation of observations of the coldest neutron stars, is produced by Cooper pairing of neutrons. This puts stringent constraints (Paper I) on the density dependence of the critical temperature $T_{\rm cnt}(\rho)$ for triplet-state neutron pairing. Tuning our phenomenological model of $T_{\rm cnt}(\rho)$ we have obtained a noticeable dependence of cooling on neutron star mass M.

In the scenario of Paper I we also needed strong proton pairing in the outer cores of neutron stars to explain the observations of neutron stars hottest for their age. In Paper II we extended that scenario taking into account the possible presence of accreted envelopes and singlet-state pairing of neutrons in the stellar crust. We have shown that the presence of accreted envelopes allows us to take weaker proton pairing. Note that models of weaker pairing are consistent with recent microscopic calculations of proton critical temperatures (Zuo et al. 2004; Takatsuka & Tamagaki 2004), although some other calculations predict much stronger proton pairing [e.g. Lombardo & Schulze (2001); see also references in Yakovlev et al. (1999), and a recent paper by Tanigawa et al. (2004)].

In this paper, for simplicity, we use the model of strong proton pairing in the stellar core. However, following Paper II, we could assume the presence of accreted envelopes, which would again allow us to weaken proton pairing. Adopting moderately strong proton pairing (with $T_{\rm cp}^{\rm max} \gtrsim 10^9$ K), we could interpret the observations of neutron stars warmest for their age.

The main feature of this paper is the consideration of EOSs that open the direct Urca process in central layers ($\rho \gtrsim 10^{15}\,{\rm g\,cm^{-3}}$) of most massive stars. We have employed the parametrization of the EOS of Akmal et al. (1998) proposed by Heiselberg & Hjorth-Jensen (1999, 2000). In combination with properly chosen phenomenological models for strong proton pairing ($T_{\rm cp}^{\rm max} \gtrsim 5 \times 10^9$ K at $\rho \lesssim 8 \times 10^{14}\,{\rm g\,cm^{-3}}$) and moderate neutron pairing ($T_{\rm cnt}^{\rm max} \sim 6 \times 10^8$ K at $\rho \gtrsim 10^{15}\,{\rm g\,cm^{-3}}$), it allows us to predict new types of cooling neutron stars, in addition to those given by the cooling scenario without any direct Urca process (Papers I and II, Section 3). They are rapidly cooling neutron stars with masses higher than the direct Urca threshold mass $M_{\rm D}$. We have shown (Section 4) that the family of these stars can be either rarely populated (Fig. 4) and thus difficult to discover, or rather distinct and populated (Fig. 6), depending on the choice of model EOS of dense matter and model for neutron superfluidity. Neutron stars from the distinct class could be cold but much warmer than massive stars with the fully open direct Urca process.

There is no clear evidence for the existence of such cold stars at the moment but it may appear in the future. For instance, low upper limits on thermal emission from hypothetical neutron stars in a few supernova remnants (Kaplan et al. 2004) can be treated as an indirect indication of the existence of such cold stars. In this context the new scenario would allow one to explain the existence of these cold objects (if discovered) in the frame of standard and simple physics of dense matter (without assuming the presence of hyperons and/or exotic forms of matter, such as pion/kaon condensates or quarks).

As has already been emphasized, we need neutron pairing to explain the current observations of stars coldest for their age. However, according to Gusakov et al. (2004b), cooling curves are not too sensitive to exchanging $T_{\rm cp}(\rho) \rightleftharpoons T_{\rm cnt}(\rho)$ in neutron star cores. Therefore, we would also be able to explain the data assuming strong neutron pairing and moderate proton pairing in stellar cores.

Finally, let us note that the same physics of neutron star interiors, which is tested by observations of isolated (cooling) neutron stars, can also be tested by observations of accreting neutron stars in soft X-ray transients (e.g. Yakovlev, Levenfish & Haensel 2003) based on the hypothesis of deep crustal heating of such stars (Brown, Bildsten & Rutledge 1988) by pycnonuclear reactions in accreted matter (Haensel & Zdunik 1990). The observations of soft X-ray transients in quiescent states indicate (Yakovlev, Levenfish & Gnedin 2005) the existence of rather cold neutron stars (first of all, SAX J1808.4−3658) inconsistent with the minimal model of cooling neutron stars. Although these observations are currently inconclusive (e.g. Yakovlev et al. 2005), if confirmed in future observations, they could give an evidence in favour of the cooling scenario proposed in this paper.

ACKNOWLEDGMENTS

We are grateful to A. Y. Potekhin for providing us with fitting parameters for the APR EOS, as well as to A. M. Krassilchtchikov and K. P. Levenfish for assistance in drawing figures. We are also grateful to the anonymous referee for critical remarks. This work has been supported partly by the RFBR (grants 05-02-16245 and 03-07-90200), by the programme Russian Leading Scientific School (grant 1115.2003.2), by the Russian Science Support Foundation, and by the INTAS (grant YSF 03-55-2397).

REFERENCES

Akmal A., Pandharipande V. R., Ravenhall D. G., 1998, Phys. Rev. C, 58, 1804 (APR)
Brown E. F., Bildsten L., Rutledge R. E., 1998, ApJ, 504, L95
Douchin F., Haensel P., 2001, A&A, 380, 151
Flowers E. G., Ruderman M., Sutherland P. G., 1976, ApJ, 205, 541
Gnedin O. Y., Yakovlev D. G., Potekhin A. Y., 2001, MNRAS, 324, 725
Gusakov M. E., Kaminker A. D., Yakovlev D. G., Gnedin O. Y., 2004a, A&A, 423, 1063 (Paper I)
Gusakov M. E., Kaminker A. D., Yakovlev D. G., Gnedin O. Y., 2004b, Astron. Lett., 30, 759
Haensel P., Potekhin A. Y., 2004, A&A, 428, 191
Haensel P., Zdunik J. L., 1990, A&A, 227, 431
Halpern J. P., Gotthelf E. V., Camilo F., Helfand D. J., Ransom S. M., 2004, ApJ, 612, 398
Heiselberg H., Hjorth-Jensen M., 1999, ApJ, 525, L45
Heiselberg H., Hjorth-Jensen M., 2000, Phys. Rep., 328, 237
Kaminker A. D., Yakovlev D. G., Gnedin O. Y., 2002, A&A, 383, 1076
Kaminker A. D., Gusakov M. E., Yakovlev D. G., Gnedin O. Y. 2005, MNRAS, submitted (Paper II)
Kaplan D. L., Frail D. A., Gaensler B. M., Gotthelf E. V., Kulkarni S. R., Slane P. O., Nechita A., 2004, ApJS, 153, 269
Kargaltsev O. Y., Pavlov G. G., Zavlin V. E., Romani R. W., 2005, ApJ, 625, 307
Lattimer J. M., Pethick C. J., Prakash M., Haensel P., 1991, Phys. Rev. Lett., 66, 2701

Lombardo U., Schulze H.-J., 2001, in Blaschke D., Glendenning N. K., Sedrakian A., eds, Physics of Neutron Star Interiors. Springer, Berlin, p. 30
McGowan K. E., Zane S., Cropper M., Kennea J. A., Córdova F. A., Ho C., Sasseen T., Vestrand W. T., 2004, ApJ, 600, 343
Motch C., Zavlin V. E., Haberl F., 2003, A&A, 408, 323
Page D., Applegate J. H., 1992, ApJ, 394, L17
Page D., Lattimer J. M., Prakash M., Steiner A. W., 2004, ApJS, 155, 623
Pavlov G. G., Zavlin V. E., 2003, in Bandiera R., Maiolino R., Mannucci F., eds, XXI Texas Symp. on Relativistic Astrophysics. World Scientific, Singapore, p. 319
Pavlov G. G., Zavlin V. E., Sanwal D., 2002, in Becker W., Lesh H., Trümper J., eds, WE-Heraeus Seminar 270, Neutron Stars, Pulsars and Supernova Remnants. MPE, Garching, p. 273
Potekhin A. Y., Yakovlev D. G., Chabrier G., Gnedin, O. Y., 2003, ApJ, 594, 404
Schwenk A., Friman B., 2004, Phys. Rev. Lett., 92, 082501
Slane P., Helfand D. J., Van der Swaluw E., Murray S. S., 2004, ApJ, 616, 403
Takatsuka T., Tamagaki R., 1997, Prog. Theor. Phys., 97, 345
Takatsuka T., Tamagaki R., 2004, Nucl. Phys. A, 738, 387
Tanigawa T., Matsuzaki M., Chiba S., 2004, Phys. Rev. C, 70, 065801
Weisskopf M. C., O'Dell S. L., Paerels F., Elsner R. F., Becker W., Tennant A. F., Swartz D. A., 2004, ApJ, 601, 1050
Yakovlev D. G., Pethick C. J., 2004, ARA&A, 42, 169
Yakovlev D. G., Levenfish K. P., Shibanov Yu. A., 1999, Sov. Phys. – Usp., 42, 737
Yakovlev D. G., Levenfish K. P., Haensel P., 2003, A&A, 407, 265
Yakovlev D. G., Levenfish K. P., Gnedin O. Y., 2005, Eur. Phys. J. A, in press (astro-ph/0501653)
Zavlin V. E., Pavlov G. G., 2004, Mem. Soc. Astron. Ital., 75, 458
Zavlin V. E., Trümper J., Pavlov G. G., 1999, ApJ, 525, 959
Zavlin V. E., Pavlov G. G., Sanwal D., 2004, ApJ, 606, 444
Zuo W., Li Z. H., Lu G. C., Li J. Q., Scheid W., Lombardo U., Schulze H.-J., Shen C. W., 2004, Phys. Lett. B, 595, 44

This paper has been typeset from a TEX/LATEX file prepared by the author.